Indian Journal of Chemistry
Vol. 60A February 2021, pp. 185-195

Synthesis, spectral and structural characterization of organic ammonium paratungstates

Sudesh M Morajkar & Bikshandarkoil R Srinivasan*
School of Chemical Sciences, Goa University, Goa 403 206, India
*E-mail: srini@unigoa.ac.in

Received 29 September 2020; revised and accepted 03 December 2020

Dissolution of tungsten(VI) oxide hydrate ($WO_3 \cdot H_2O$) in aqueous organic amine (RNH_2 where R = methyl or ethyl, or *n*-propyl or isopropyl or *n*-butyl or *t*-butyl etc.) results in the formation of the tetrahedral tetraoxidotungstate(VI) species in solution. Slow evaporation of the reaction mixture to isolate the tetraoxidotungstates charge balanced by organic ammonium cations afforded organic ammonium paratungstates having formula $(RNH_3)_{10}[H_2W_{12}O_{42}] \cdot xH_2O$. The presence of $(WO_4)^{2-}$ species in solution and the $[H_2W_{12}O_{42}]^{10-}$ unit in the solid product is confirmed by the characteristic Raman spectra. In this paper, we report on the synthesis, Raman spectra, crystal structures and properties of two organic ammonium paratungstates *viz*. $(MeNH_3)_{10}[H_2W_{12}O_{42}] \cdot 12H_2O$ **1** ($MeNH_2$ = methylamine) and $(EtNH_3)_{10}[H_2W_{12}O_{42}] \cdot 4H_2O$ **2** ($EtNH_2$ = ethylamine). Thermal decomposition of **1** or **2** at 800 °C results in the formation of monoclinic form of tungsten trioxide WO_3. A comparative study of several paratungstates is described.

Keywords: Tetraoxidotungstate, Organic amine, Paratungstate, Raman spectra, Crystal structure

The study of tungsten and its compounds commenced more than two centuries ago after the discovery of a new oxide from the mineral scheelite by the Swedish chemist Scheele in 1781[1]. In a paper titled "*Ueber das Wolfram*", Wöhler[2] reported a method for the preparation of tungstic acid *viz*. hydrated tungsten trioxide and other W compounds. Since then several papers reporting on the composition of the compounds derived from tungsten trioxide (WO_3) have appeared in the older literature[3-11]. The several crystalline tungstates reported till about 1950 were grouped by Saddington and Cahn[11] into three classes in a paper reporting on the formula of hydrated sodium paratungstate. In terms of composition the known tungsten compounds were classified as i) normal tungstates whose aqueous solutions are alkaline and contain WO_3:R_2O in 1:1 mole ratio (R is Na^+ or $(NH_4)^+$ or any monocation); ii) acidic paratungstates were formulated as $7WO_3 \cdot 3R_2O \cdot xH_2O$ by some authors[3,4] and $12WO_3 \cdot 5R_2O \cdot xH_2O$ by others[5,7,8] and iii) metatungstates for which a 4:1 ratio of WO_3:R_2O was proposed. Despite an incorrect formulation of metatungstate, the Saddington and Cahn paper did resolve the composition of sodium paratungstate as containing W:Na in 12:10 ($12WO_3$:$5Na_2O$) ratio ruling out the $7WO_3 \cdot 3Na_2O$ composition. The formula of sodium paratungstate was proposed as $Na_{10}W_{12}O_{41} \cdot 28H_2O$ based on unit cell and analytical data[11]. However, this composition was different from that of paramolybdate, the ammonium salt of which was formulated as $(NH_4)_6[Mo_7O_{24}] \cdot 4H_2O$ by Sturdivant[12] based on a unit cell determination.

The importance of these compounds was realized in the 1950s and the iso- and heteropoly acids and the salts of V, Mo, W etc. were considered as special compounds in the handbook of preparative inorganic chemistry by Brauer[13]. Currently similar compounds of the early transition metals V, Mo, W etc. referred to by the term polyoxometalate are described in all standard text books[1,14]. The chemistry of polyoxometalates (POMs) is a widely studied research area as evidenced by several publications in recent years[15-20]. Among the POMs, the isopolyanions of tungsten are well known of which paratungstate (*vide infra*) is extensively studied. The paratungstates of sodium and ammonium deserve mention, as a study of these compounds containing several W atoms bonded to O atoms was crystallographically challenging in the 1950s. It took almost three decades and the efforts of several researchers[21-26] (See Supplementary data) starting from Lindqvist[21,22] followed by Lipsomb[23], Weiss[24], Allmann[25], Evans and Prince[26] to correctly confirm the formula of paratungstate ion as $[H_2W_{12}O_{42}]^{10-}$ in accordance with a W:Na ratio of 12:10 first proposed by Cahn and Saddington[11].

A number of paratungstates charge balanced by a variety of counter cations for example $Mg_5[H_2W_{12}O_{42}]\cdot 38H_2O$[27] and $Na_5Fe_{2.5}[H_2W_{12}O_{42}]\cdot 36H_2O$[28] have been structurally characterized and are archived in the Cambridge Structural Database (CSD)[29] and Inorganic Chemistry Structure Database (ICSD)[30]. Unlike the term 'paratungstate' which refers to the species $[H_2W_{12}O_{42}]^{10-}$ paramolybdate[12,22,31] refers to $[Mo_7O_{24}]^{6-}$. Presently there are two types of paratungstates namely paratungstate A[32,33] formulated as $[W_7O_{24}]^{6-}$ and paratungstate B formulated as $[H_2W_{12}O_{42}]^{10-}$. Paratungstate B[28] is also referred to as dodecatungstate as it contains twelve tungsten atoms in its formula unit. Another polyoxotungstate anion with twelve tungsten atoms *viz.* metatungstate $[H_2W_{12}O_{40}]^{6-}$ is also known[1,14]. Although the terms dodecatungstate / paratungstate B, metatungstate do not give any information about the number and type of oxygen atoms in the polyanions, these terms are preferred to refer to these species, instead of the very long IUPAC names[34] dihydrogendotetracontaoxo dodecatungstate(10-) and dihydrogentetracontaoxo-dodecatungstate(6-), respectively, for $[H_2W_{12}O_{42}]^{10-}$ and $[H_2W_{12}O_{40}]^{6-}$.

Generally, paratungstates are prepared by the acidification of an aqueous solution of $Na_2WO_4\cdot 2H_2O$ in the presence of appropriate counter cation. Acidification leads to the condensation of monomeric tetrahedral $\{WO_4\}$ units to form higher nuclearity polyoxotungstates. A survey of the literature reveals that only one example of an organic paratungstate[35] is known to date. In view of this we have undertaken this work to prepare organic ammonium paratungstates by investigating the reaction of hydrated tungsten trioxide in aqueous organic amine solutions. In this study we have employed Raman spectroscopy to characterize the species in the reaction medium and the final solid product, as described recently for the study of WO_3/ammonia/water reaction system[36]. The results of these investigations showing the usefulness of Raman technique for product characterization and the crystal structures of two new organic ammonium paratungstates are described in this report.

Materials and Methods

All the chemicals used in this study were of reagent grade and were used as received from commercial sources without any further purification. Tungsten trioxide hydrate ($WO_3\cdot H_2O$) marketed by Thomas Baker Chemicals Private Limited under the name tungstic acid (98% purity) was used as W source. Infrared (IR) spectra of the solid samples diluted with KBr were recorded on a Shimadzu (IR Prestige-21) FT-IR spectrometer from 4000-400 cm^{-1} at a resolution of 4 cm^{-1}. Ammonium paratungstate tetrahydrate was prepared by a slight modification of the literature procedure[13] and used as a reference compound for Raman spectral analysis of organic paratungstates. Raman spectra of compounds in solid-state and in aqueous medium were recorded by using an Agiltron PeakSeeker Pro Raman instrument with 785 nm laser radiation for excitation and laser power set to 100 mW. The samples for solution Raman spectra were taken in a quartz cuvette. Isothermal weight loss studies were performed in a temperature controlled electric furnace. Simultaneous thermogravimetry (TG) and differential thermal analyses (DTA) of a powdered sample of **1** and **2** were performed in alumina crucible in the temperature range of 30 °C to 600 °C, using a Netzsch STA-409 PC thermal analyzer, at a heating rate of 10 °C/min. X-ray powder patterns were recorded on a Rigaku Miniflex II powder diffractometer using Cu-Kα radiation with Ni filter. Conductivity measurements of **1** and **2** were carried out at room temperature using a Digital conductivity meter (LT-16) from Labtronics equipped with a standard conductometric cell composed of two platinum black electrodes.

Synthesis of ammonium paratungstate[13] $(NH_4)_{10}[H_2W_{12}O_{42}]\cdot 4H_2O$

Tungsten(VI) oxide hydrate (2.49 g, 10 mmol) was dissolved in excess liquor ammonia solution and the mixture was stirred well. The reaction mixture containing a small amount of insoluble matter was filtered to obtain a clear solution, which exhibits an intense Raman signal at 928 cm^{-1}. The clear filtrate was left aside undisturbed to obtain colourless crystalline solid, which was isolated by filtration. Yield 2.26 g.

IR data (cm^{-1}) : 3868-2414 (broad), 1646, 1414, 933, 878, 550, 495; Raman data (cm^{-1}) : 946, 865, 796, 666, 350, 320.

Synthesis of $(MeNH_3)_{10}[H_2W_{12}O_{42}]\cdot 12H_2O$ 1 and $(EtNH_3)_{10}[H_2W_{12}O_{42}]\cdot 4H_2O$ 2

To a suspension of tungsten(VI) oxide hydrate (2.49 g, 10 mmol) in 10 mL of water, 40% methylamine (5 mL) was added in excess. The resultant reaction mixture was stirred well to dissolve the tungsten trioxide completely. The almost clear solution (pH = ~ 12) was then filtered and kept undisturbed for crystallization. After a week crystals were obtained. At this point the pH was around 6.9. The crystals were isolated and dried in air to afford 2.14 g of $(MeNH_3)_{10}[H_2W_{12}O_{42}]\cdot 12H_2O$ **1**.

The use of 70% ethylamine (~5 mL) in the above reaction in place of methylamine afforded 2.28 g of $(EtNH_3)_{10}[H_2W_{12}O_{42}]\cdot 4H_2O$ **2**.

Compound **1** = IR data (cm^{-1}) : 3788-2639 (broad), 2764, 2557, 2011, 1615, 1483, 1425, 1260, 929, 880, 707, 491; Raman data (cm^{-1}) : 1454, 941, 846, 801, 325; DTA (°C) : 93 (endo), 255 (endo), 334 (exo), 513 (exo).

Compound **2** = IR data (cm^{-1}) : 3730-2259 (broad), 2887, 2805, 2624, 2532, 2087, 1607, 1483, 1401, 1327, 1202, 1054, 929, 882, 705, 558, 500; Raman data (cm^{-1}) : 1454, 941, 846, 801, 325; DTA (°C) : 93 (endo), 255 (endo), 355 (exo), 513 (exo).

Raman spectral investigations of aqueous organic amine solutions of tungstic acid monohydrate

To about 1.0 g of a commercial sample of tungsten(VI) oxide hydrate ($WO_3\cdot H_2O$) in ~10 mL water, a slight excess (~5 mL) of organic amine RNH_2 (R = methyl or ethyl, or *n*-propyl or isopropyl or *n*-butyl or *t*-butyl or *sec*.-butyl or trimethyl or triethyl) was added. The reaction mixture was stirred well to obtain a clear solution. The solution was filtered and the clear filtrate was investigated by Raman spectrum. The reaction mixture was left undisturbed for crystallization. On evaporation of the solvent, a colourless crystalline solid, which exhibits a strong Raman signal at 941 cm^{-1} was obtained (For complete details see Supplementary Data).

X-ray crystal structure determination

For compounds **1** and **2** single crystal X-ray study was performed at the Sophisticated Analytical Instrument Facility, Indian Institute of Technology, Madras. X-ray data were collected using a Bruker AXS Kappa Apex II CCD Diffractometer equipped with graphite monochromated Mo (Kα) (λ = 0.7107 Å) radiation. The structures were solved by direct methods using SIR92[37] and refined by full-matrix least squares techniques using SHELXL-2014[38]. All non-hydrogen atoms were refined anisotropically. The H atoms attached to methylamine cations and water molecules in **1** and the nonlabile H atoms in the paratungstate anion of both **1** and **2** could not be located. Technical details of data acquisition and selected refinement results are listed in Table 1.

Results and Discussion

Synthetic aspects, spectral, thermal and conductivity studies

In this work, tungsten trioxide hydrate ($WO_3\cdot H_2O$) was used as W source for the synthesis of the organic ammonium paratungstates. In our studies of organic ammonium polyoxomolybdates, we have shown that molybdenum trioxide (MoO_3) can be dissolved in excess aqueous *n*-butylamine to obtain tetrahedral $(MoO_4)^{2-}$ species, which on slow evaporation afforded a mixed monomolybdate-heptamolybdate compound charge balanced by *n*-butylammonium cations[39]. In view of the paucity of organic ammonium paratungstates in the literature, we investigated the room temperature reaction of hydrated tungsten trioxide with several organic amines *viz*. methylamine, ethylamine, propylamine, isopropylamine, *n*-butylamine, *sec*-butylamine, *t*-butylamine, trimethylamine and triethylamine. As in the case of Mo, tungsten trioxide dissolves in excess amine RNH_2 (R = methyl or ethyl, or *n*-propyl or isopropyl or *n*-butyl or *t*-butyl or *sec*.-butyl or trimethyl or triethyl) to afford a clear reaction mixture (pH = ~ 12). The clear solution thus obtained showed a strong Raman signal at 928 cm^{-1} assignable for the symmetric stretching vibration of the $(WO_4)^{2-}$ species in solution[40] (Fig. 1). Slow evaporation of the alkaline reaction mixture resulted in a decrease in the pH due to the volatility of the amines. In a week's time, the pH of the reaction mixture became weakly acidic (pH~ 6.9) accompanied by the formation of a colourless solid. The Raman spectra of all the products are nearly similar and show the absence of the 928 cm^{-1} signal of $(WO_4)^{2-}$. For all products an intense Raman band was observed at 941 cm^{-1} and the spectra are nearly identical with the spectrum of the reference compound viz. ammonium paratungstate tetrahydrate (Fig. 1). The Raman spectral results are identical to the behavior observed by us for the WO_3/ammonia/water reaction system[36]. The signal at 941 cm^{-1} can be assigned for the symmetric stretching vibration of the $\{WO_6\}$ unit (Supplementary Data, Scheme S1). Thus, the Raman spectral study provides a clue for the condensation of $(WO_4)^{2-}$ species as the evaporation proceeds resulting in lowering of pH accompanied by the formation of paratungstate polyanion. The crystalline products obtained for methyl and ethylamine (compounds **1** and **2**,

Table 1 — Crystal data and structure refinement for compound **1** and **2**

Empirical formula	$C_{10}H_{86}N_{10}O_{54}W_{12}$ **1**	$C_{20}H_{90}N_{10}O_{46}W_{12}$ **2**
Formula weight	3417.08	3413.21
Temperature	296(2) K	296(2) K
Wavelength	0.71073 Å	0.71073 Å
Crystal system, Space group	Triclinic, $P\bar{1}$	Monoclinic, *C2/c*
Unit cell dimensions	a = 9.5603(6) Å	a = 21.559(2) Å
	b = 13.0649(9) Å	b = 15.6782(17) Å
	c = 13.5403(9) Å	c = 19.531(2) Å
	α= 72.223(4)°	α= 90°
	β= 89.951(4)°	β= 90.245(5)°
	γ = 86.361(4)°	γ = 90°
Volume	1606.94(19) $Å^3$	6601.4(13) $Å^3$
Z, calculated density	1, 3.531 mg m^{-3}	4, 3.434 mg m^{-3}
Absorption coefficient	21.489 mm^{-1}	20.915 mm^{-1}
F(000)	1536	6144
Crystal size	0.500 x 0.100 x 0.100 mm^3	0.100 x 0.100 x 0.050 mm^3
θ range for data collection	2.603 to 24.997°	1.043 to 24.998°
Index ranges	$-11 \leq h \leq 11, -15 \leq k \leq 15, -16 \leq l \leq 16$	$-25 \leq h \leq 25, -18 \leq k \leq 18, -23 \leq l \leq 23$
Reflections collected / unique	18444 / 5651 [R(int) = 0.0592]	47812 / 5812 [R(int) = 0.1346]
Observed reflection	7684	4114
Completeness θ = 24.997°	99.60%	99.90%
Absorption correction	Semi-empirical from equivalents	Semi-empirical from equivalents
Refinement method	Full-matrix least-squares on F^2	Full-matrix least-squares on F^2
Data / restraints / parameters	5651 / 35 / 388	5812 / 249 / 421
Goodness-of-fit on F^2	1.133	1.168
Final R indices [$I>2\sigma(I)$]	R1 = 0.0474, wR2 = 0.1067	R1 = 0.0881, wR2 = 0.2017
R indices (all data)	R1 = 0.0611, wR2 = 0.1120	R1 = 0.1200, wR2 = 0.2267
Largest diff. peak and hole	3.076 and -2.462 e.$Å^{-3}$	3.826 and -4.591 e.$Å^{-3}$
CCDC No.	2016772	2016773

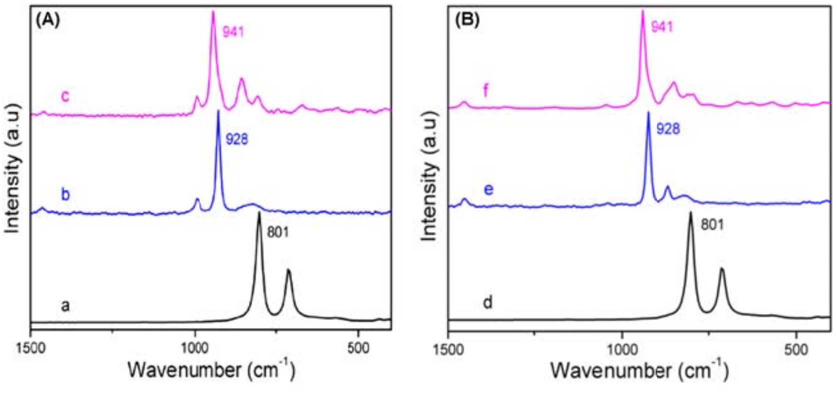

Fig 1 — Raman spectra of ($WO_3{\cdot}H_2O$) (**a**), reaction mixture of ($WO_3{\cdot}H_2O$) with methylamine (**b**) and $(MeNH_3)_{10}[H_2W_{12}O_{42}]{\cdot}12H_2O$ **1** (**c**) (**A**) and ($WO_3{\cdot}H_2O$) (**d**), reaction mixture of ($WO_3{\cdot}H_2O$) with ethylamine (**e**) and $(EtNH_3)_{10}[H_2W_{12}O_{42}]{\cdot}4H_2O$ **2** (**f**) (**B**)

respectively) have been structurally characterized by single crystal method. Due to the inability to obtain suitable crystals for X-ray structure work, the colourless product was characterized as hydrated organic paratungstate by Raman (Supplementary Data, Fig. S1) and IR studies (Supplementary Data, Fig. S2) for the other amines.

The IR spectra of all compounds including **1** and **2** exhibit several signals in the mid IR region indicating the presence of organic cation (Supplementary Data, Fig. S2). The broad absorption seen around 3500 cm^{-1} can be attributed to the O-H stretching vibration of water molecules and N-H of organic ammonium cation. The presence of water and protonated amine can also be evidenced by bands at 1615 and 1425 cm^{-1} for **1** and 1607 and 1401 cm^{-1} for **2** assignable to O-H and N-H bending vibrations, respectively. The symmetric stretching vibration υ_1 of the WO_6 unit is observed as an intense band in the Raman spectrum at 941 cm^{-1} while the band at 929 cm^{-1} in **1** and **2** can be assigned for terminal W-O vibrations. The IR spectra of the other organic ammonium paratungstates are very nearly similar as observed for the Raman spectra. The phase purity of the compounds **1** and **2** were confirmed by comparing experimental X-ray powder pattern with that calculated from single crystal data (Supplementary Data, Fig. S3).

The thermal studies of **1** and **2** show nearly similar mass loss pattern as evidenced by an endothermic event at 93 °C in the DTA curve (Figs 2-3) accompanied by a weight loss of 5.76 % in **1** and 1.85 % in **2** assignable for the loss of twelve and four water molecules respectively. Above 200 °C the DTA curve shows an endothermic (255 °C for **1** and **2**) and two exothermic (334, 513 °C for **1** and 355, 513 °C for **2**) peaks which can be attributed to the decomposition of the organic paratungstate resulting in a residue of 80.54 % for **1** and 81.72 % for **2**. The residual mass obtained is in close agreement with the calculated residue (81.42 % for **1** and 81.51 % for **2**) for formation of tungsten trioxide (WO_3). The results obtained are in accordance with the pyrolysis experiment of **1** and **2** carried out in a furnace.

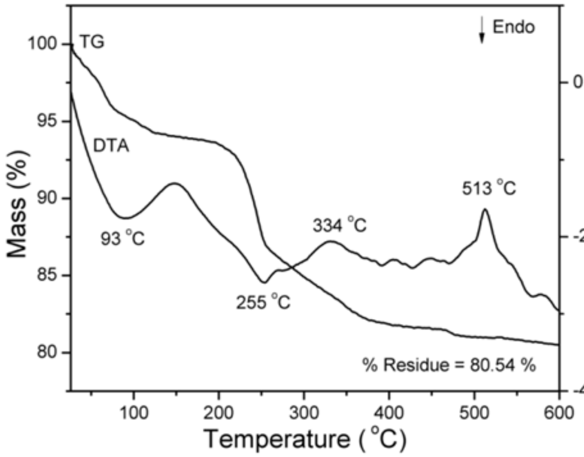

Fig. 2 — TG-DTA curves of $(MeNH_3)_{10}[H_2W_{12}O_{42}]\cdot 12H_2O$ **1**

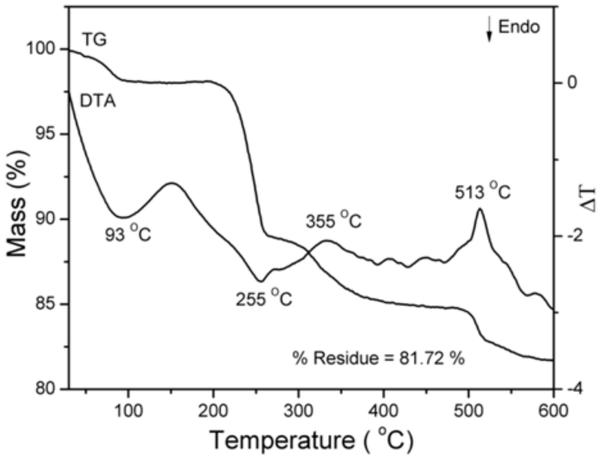

Fig. 3 — TG-DTA curves of $(EtNH_3)_{10}[H_2W_{12}O_{42}]\cdot 4H_2O$ **2**

The powder pattern of residual oxide obtained by heating **1** (or **2)** (Fig. 4) at 800 °C for 2 h in a temperature controlled furnace is in agreement with the powder pattern of monoclinic form of WO_3 reported by Tanisaki[41]. This WO_3 modification crystallizing in the monoclinic $P2_1/n$ space group was prepared by heating purified wolframic acid (tungstic acid) in a silica tube at 1300 °C for several hours[42]. However, in the present work we have obtained the monoclinic form of crystalline WO_3 at a considerably lower temperature (800 °C) by pyrolysis of **1** or **2**. A hexagonal form of WO_3 was reported by dehydration of $WO_3\cdot 1/3H_2O$[43]. A hydrothermal synthesis of the hexagonal or pyrochlore forms of WO_3 has also been reported[44]. It is to be noted that WO_3 can exist in several polymorphic modifications[45]. The molar conductivity of aqueous solutions of **1** and **2** exhibit a steady increase with dilution (Table 2) indicating facile dissociation of **1** and **2** in dilute solution producing $[H_2W_{12}O_{42}]^{10-}$ ions and protonated amines which is in accordance with the crystal structure (*vide infra*) of **1** and **2** showing discrete ions.

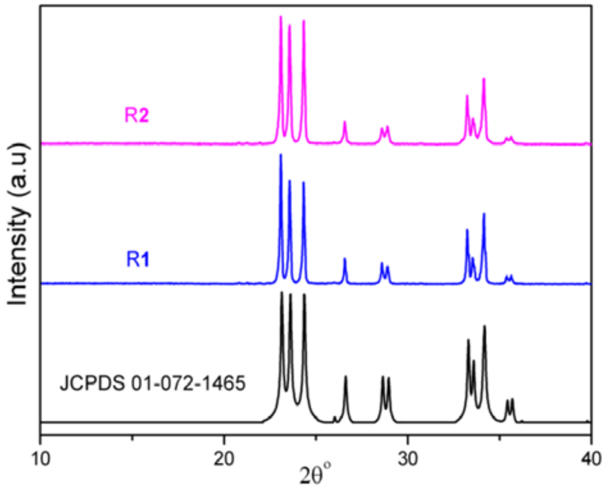

Fig. 4 — X-ray powder patterns of monoclinic WO_3 (JCPDS 01-072-1465)[41] (**bottom**), residue obtained after pyrolysis of $(MeNH_3)_{10}[H_2W_{12}O_{42}]\cdot 12H_2O$ **1** (**R1**) and $(EtNH_3)_{10}[H_2W_{12}O_{42}]\cdot 4H_2O$ **2** (**R2**) at 800 °C

Description of the crystal structure of 1 and 2

Compound **1** crystallizes in the centrosymmetric triclinic space group $P\bar{1}$ and its crystal structure consists of a paratungstate $[H_2W_{12}O_{42}]^{10-}$ anion located on an inversion centre (Fig. 5), five unique methylammonium $(MeNH_3)^+$ cations (N1 to N5), and six crystallographically independent water molecules (O22 to O27) (Supplementary Data, Fig. S4). The midpoint of the line connecting W1 and W1^i or O10 and O10^i or for that matter the midpoint between any atom and its symmetry generated counterpart is the centre of inversion (Supplementary Data, Fig. S4). In view of the centrosymmetric nature of the paratungstate ion, the asymmetric unit of **1** is a half of the formula unit, with the other half being symmetry generated. The C-N bond distances of the organic cations are in the normal range (Supplementary Data, Table S1). The hydrogen atoms attached to the carbon and nitrogen atoms of the unique methylammonium cations could not be located. The inability to locate the H atoms of the lattice water molecules precludes a discussion of hydrogen bonding in **1**. The W-O bond lengths and O-W-O bond angles of the paratungstate anion (Supplementary Data, Table S1) are in normal range and are in agreement with reported data[29]. The centrosymmetric $[H_2W_{12}O_{42}]^{10-}$ anion (Fig. 5) in both the compounds (**1** and **2)** is built up of four trimetallic edge sharing units which can be divided into two types i) triangular cap type $\{W_3O_{13}\}$ and ii) open angular trimer $\{W_3O_{14}\}$. Each trimeric unit is formed by three edge sharing $\{WO_6\}$ octahedra. Capped $\{W_3O_{13}\}$ unit is formed by three edge sharing $\{WO_6\}$ octahedra with a common μ_3-oxygen atom. In contrast, open angular trimer $\{W_3O_{14}\}$ unit is made up of linearly linked $\{WO_6\}$ octahedra to each other without sharing a common oxygen atom. Furthermore, each $\{WO_6\}$ octahedron in $\{W_3O_{13}\}$ has one terminal O atom whereas $\{W_3O_{14}\}$ contains two terminal O atoms per $\{WO_6\}$ octahedron. The O atoms of paratungstate anion can be classified into three different categories namely a) eighteen terminal O atoms (O_t) connected to the W centre b) eighteen μ_2-bridging bidentate O atoms and c) six μ_3-bridging tridentate O atoms. Bidentate and tridentate O atoms are sub divided in two categories, one category bridges the W atoms within the same $\{W_3O_{13}\}$ or $\{W_3O_{14}\}$ units while the other bridges W atoms in different trimeric units.

Table 2 — Specific conductivity (Ꝁ) and molar conductivity (λ_m) of **1** and **2**

Conc. (M)	Specific conductivity (Ꝁ) (S cm^{-1})		Molar conductivity (λ_m) (S cm^2 mol^{-1})	
	1	**2**	**1**	**2**
0.1	0.0133	0.0129	133	129
0.08	0.0125	0.0118	156	147
0.06	0.0117	0.0107	192	179
0.04	0.0105	0.0094	262	235
0.02	0.0082	0.0079	411	393

Compound **2** crystallizes in the centrosymmetric monoclinic space group *C2/c*. The crystal structure consists of an unique paratungstate $[H_2W_{12}O_{42}]^{10-}$ anion with the W1 and W7 atoms located on a twofold axis, five crystallographically independent ethylammonium cations, and two unique lattice water molecules (Fig. 6). Seven unique W atoms (W1 to W7) and twenty one unique oxygen atoms (O1 to O21) are sufficient to describe the centrosymmetric paratungstate $[H_2W_{12}O_{42}]^{10-}$ anion, in view of the special position of W1 and W7. Twenty one oxygen

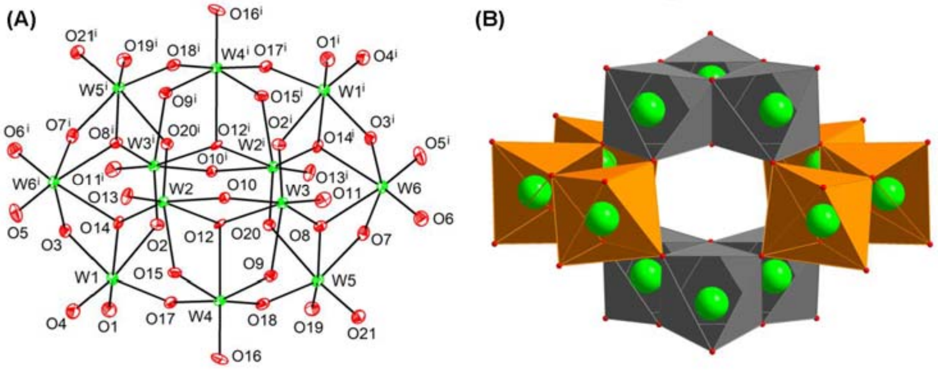

Fig. 5 — The atom-labelling scheme for the centrosymmetric $[H_2W_{12}O_{42}]^{10-}$anion in **1**. Midpoint between O10 and O10^i is the inversion centre (see also Fig S4). Displacement ellipsoids are drawn at 30% probability level. Symmetry code: i) -x+1,-y+2,-z+1 (**A**). A polyhedral representation of $[H_2W_{12}O_{42}]$ anion in $(MeNH_3)_{10}[H_2W_{12}O_{42}]\cdot12H_2O$ **1.** Colour code: $\{W_3O_{14}\}$ are orange octahedra and $\{W_3O_{13}\}$ are grey octahedra (**B**)

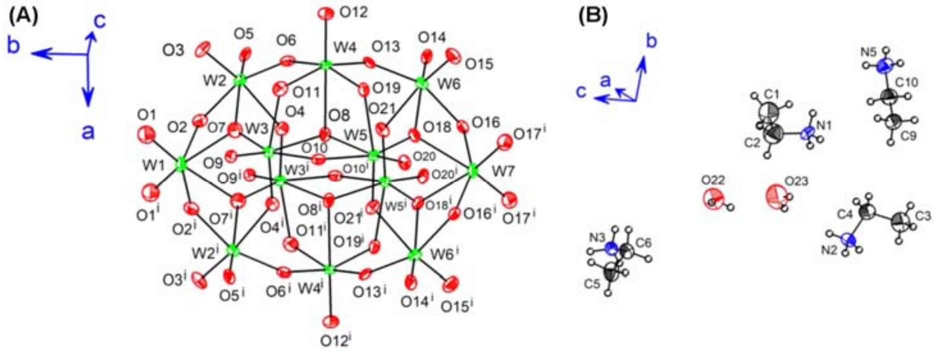

Fig. 6 — The atom labelling scheme for the centrosymmetric $[H_2W_{12}O_{42}]^{10-}$ anion in **2**. W1 and W7 are on a two-fold axis (**A**). The unique ethylammonium cations $(EtNH_3)^+$ and lattice water molecules of **2** (**B**). Displacement ellipsoids are drawn at 30% probability except for the H atoms, which are shown as spheres of arbitrary radii. Symmetry code: -x+1, y, -z+1/2

atoms ($O1^i$ to $O21^i$) and five W atoms ($W2^i$-$W6^i$) are symmetry generated by the two fold axes. In view of the centrosymmetric anion, the asymmetric unit contains only five unique ethylammonium cations and two lattice water molecules (Fig. 6). The C-C and C-N bond distances of the organic cations are in the normal range (Supplementary Data, Table S2). The W-O bond length and O-W-O bond angles of the paratungstate anion agree well with reported data and are comparable to those observed for **1** (Supplementary Data, Table S2).

An analysis of the crystal structure of **2** reveals that the $(EtNH_3)^+$ cations, $[H_2W_{12}O_{42}]^{10-}$ and water molecules are interlinked by three types of hydrogen bonding interactions viz. O-H···O, N-H···O and C-H···O (Table 3). The oxygen atoms of the unique $[H_2W_{12}O_{42}]^{10-}$ anion and water molecules function as H- acceptors. All of the H atoms linked to the oxygen atoms of the lattice water, some of the H atoms bonded to the carbon of the organic cation (C4, C5, C6, C7 and C10) and all of the H atoms attached to the nitrogen atoms of the organic cations act as H donors. The organic cations are hydrogen bonded to paratungstate with the aid of N-H···O and C-H···O interactions. For example, the unique cation N1 and N2 are hydrogen bonded to three and two symmetry related paratungstate anions respectively (Fig. 7) while each of the cation N3, N4 and N5 is linked to two symmetry related paratungstates (Supplementary Data, Fig. S5). The O22-H22A···O23 interaction between the lattice water molecules O22 and O23 result in the formation of a water dimer (Fig. 8). The water dimer is further hydrogen bonded to two symmetry related paratungstate anions with the aid of four O-H···O interactions and three symmetry related cations with the aid of two N-H···O and one C-H···O hydrogen bonds. These interactions result in the formation of a two-dimensional network (Fig. 8) showing that the lattice water interlinks the cations and anions.

Chemistry of formation of 1 and 2

Retrosynthetic analysis is a well-known concept in organic synthesis. In recent years Ramanan and coworkers[46] have shown that retrosynthesis of a crystal structure can be used to obtain valuable insights for the synthesis of coordination compounds by considering a crystal as a supermolecule and crystallization as a supramolecular reaction[47]. Ramanan[46] has demonstrated that the retrosynthesis of a crystal structure can suggest the species / units involved in the supramolecular aggregation, since nucleation of a crystal occurs from chemically reasonable molecules or tectons which interact in the solution at supersaturation. Following this approach we have performed a retrosynthetic analysis of the formation of **1** or **2** and the following are our findings. The dissolution of tungsten trioxide hydrate in excess aqueous organic amine results (Step 1, Scheme 1) in the formation of the tetrahedral $(WO_4)^{2-}$ species as confirmed by the characteristic Raman signal. The reaction medium contains W:organic ammonium cation in 1:2 ratio, in addition to the unreacted organic amine. At this stage the medium is rich in organic amine which is evidenced by the alkaline pH of the reaction medium. However, leaving the solution undisturbed does not result in the crystallization of the expected bis(organic ammonium) tetraoxido-tungstate product viz. $(RNH_3)_2(WO_4)$. Instead the product obtained is a paratungstate $(RNH_3)_{10}[H_2W_{12}O_{42}]\cdot xH_2O$ in all cases with W:organic amine in 12:10 ratio. Compounds **1** or **2** contain less than one amine per W and are amine

Table 3 — Geometric parameters (Å, °) of C–H···O, N–H···O and O–H···O hydrogen bonds in **2**

D-H	d(D-H)	d(H···A)	<(DHA)	d(D···A)	A	Symmetry codes
N1-H1A	0.89	1.87	161.9	2.73(5)	O17	x, y+1, z
N1-H1B	0.89	2.00	175	2.89(4)	O12	-x+1/2, y+1/2, -z+1/2
N1-H1C	0.89	1.84	168.3	2.72(5)	O1	-x+1, y, -z+1/2
C4-H4A	0.97	2.54	149.6	3.42(6)	O1	-x+1, y, -z+1/2
C5-H5A	0.96	2.66	112.7	3.16(8)	O23	-x+1/2, y-1/2, -z+3/2
C5-H5C	0.96	2.58	171.3	3.53(7)	O11	x, y, z+1
C6-H6A	0.97	2.63	123.5	3.27(5)	O13	x, -y, z+1/2
C6-H6B	0.97	2.4	126.7	3.08(5)	O14	x, -y, z+1/2
C7-H7A	0.96	2.6	163.8	3.53(7)	O1	x, -y+1, z+1/2
C10-H10B	0.97	2.49	133.9	3.24(6)	O12	-x+1/2, y+1/2, -z+1/2
N2-H2C	0.89	1.93	156.8	2.77(4)	O11	
N2-H2D	0.89	1.9	151.4	2.72(4)	O15	-x+1/2, y+1/2, -z+1/2
N2-H2E	0.89	1.9	156.9	2.74(5)	O3	
N3-H3D	0.89	1.92	166.1	2.79(4)	O10	x, y, z+1
N3-H3E	0.89	2.5	131.6	3.16(5)	O14	x, -y, z+1/2
N3-H3E	0.89	2.54	138.7	3.27(4)	O21	x, -y, z+1/2
N3-H3F	0.89	2.44	147.6	3.22(4)	O4	x, -y, z+1/2
N3-H3F	0.89	2.2	138.6	2.93(5)	O5	x, -y, z+1/2
N4-H4C	0.89	2.27	150.1	3.07(5)	O2	x, -y+1, z+1/2
N4-H4C	0.89	2.23	117.9	2.77(4)	O9	-x+1, -y+1, -z+1
N4-H4D	0.89	2.23	168.6	3.10(5)	O14	-x+1,y+1,-z+3/2
N4-H4E	0.89	1.96	144.2	2.73(5)	O20	x, y+1, z+1
N5-H5D	0.89	2.03	162.5	2.89(6)	O17	x, y+1, z
N5-H5D	0.89	2.59	120.2	3.13(5)	O18	x, y+1, z
N5-H5E	0.89	2.48	142.7	3.23(5)	O19	x, y+1, z
N5-H5E	0.89	2.48	132.2	3.15(8)	O23	-x+1/2, y+1/2, -z+1/2
N5-H5F	0.89	2.06	150.6	2.87(7)	O22	x, -y+1, z-1/2
O22-H22A	0.850(10)	2.00(3)	139(12)	2.70(8)	O23	
O22-H22B	0.850(10)	2.10(3)	137(7)	2.78(5)	O5	
O23-H23A	0.850(10)	2.00(3)	151(13)	2.78(6)	O3	
O23-H23B	0.850(10)	2.00(3)	152(12)	2.78(5)	O19	-x+1/2, y+1/2, -z+1/2

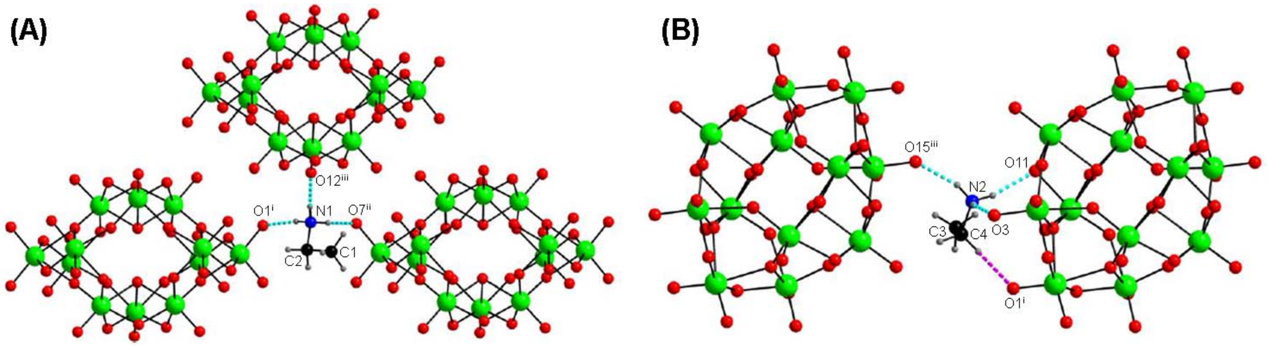

Fig. 7 — Hydrogen bonding scheme around ethylammonium cation 'N1' (**A**) and 'N2' (**B**) showing N-H···O (cyan) and C-H···O (pink) interactions in $(EtNH_3)_{10}[H_2W_{12}O_{42}]\cdot 4H_2O$ **2**, (For symmetry relations, see Table 2)

deficient products. In this context it is useful to mention that polyoxotungstates are normally isolated from acidic medium[1,14] for example by acidification of an aqueous sodium tungstate solution. However, in the present synthesis no external acid was employed. The volatility of the organic amines employed in this work resulted in an acidic medium necessary for the nucleation of polyoxotungstate providing the organic cations. The organic cations have been confirmed by structure charcterization of **1** and **2**. In the reaction medium several soluble polyoxotungstates are formed and paratungstate is one among them. Under our reaction conditions viz. slow evaporation and no external acidification, the crystallized product in all the

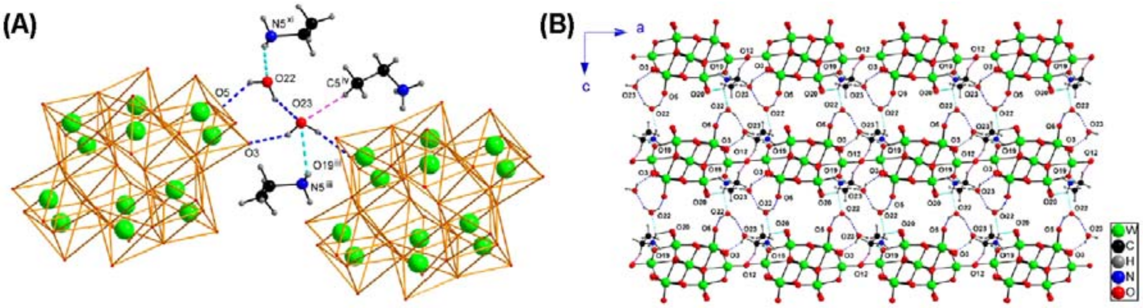

Fig. 8 — Hydrogen bonding scheme around lattice water molecules in $(EtNH_3)_{10}[H_2W_{12}O_{42}]\cdot4H_2O$ **2**, showing the water dimer (O22 and O23) (**A**). The water dimer links cations and anions into a layer. (**B**) (For symmetry relations, see Table 2)

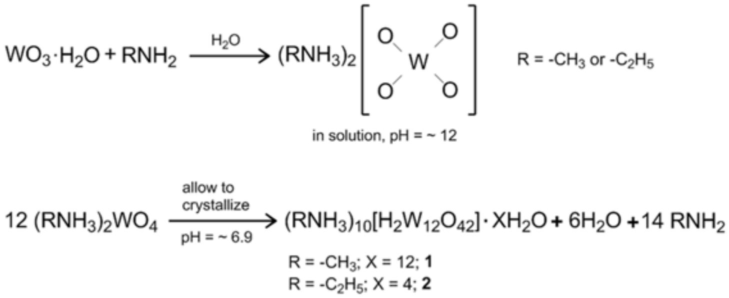

Scheme 1 — Chemistry of formation of **1** or **2**

cases is a paratungstate as evidenced by the identical Raman spectra for all products and the structural characterization of two paratungstates. Since an excess of amine was used to dissolve the WO_3 in each reaction, we propose that the key step for the formation of the final paratungstate $\{W_{12}\}$ product is the loss of fourteen moles of organic amine per mole of paratungstate formed (Step 2, Scheme 1) making the medium acidic to transform the tetrahedral $(WO_4)^{2-}$ units into the interlinked $\{WO_6\}$ octahedra in the product.

Comparative study of paratungstates

Unlike paratungstate B $[H_2W_{12}O_{42}]^{10-}$, several of which are known only one example of a structurally characterized paratungstate A[33] compound has been reported to date. The availability of several structurally characterized paratunsgates (viz. paratungstate B) in the CSD and ICSD permits a comparative discussion, the details of which are described herein. A perusal of the entries in Supplementary Data, Table S3 reveals the flexibility of the paratungstate B ion to exist in a variety of structural environments. Based on the charge balancing cations for the entries in Supplementary Data, Table S3, the paratungstates can be classified under three groups namely organic ammonium paratungstates (entry nos 1-3), metal-organic paratungstates (entry no. 4 to 21), all-inorganic paratungstates (entry nos. 22 to 81) wherein the cations do not contain any carbon. The all-inorganic compounds are archived in the ICSD[30]. It is interesting to note that all structurally characterized paratungstates contain at least one lattice water molecule. A perusal of the space groups reveal that a majority of the compounds crystallize in centrosymmetric space groups while only a few are non-centrosymmetric (entry no 75 to 81). In all the compounds listed in Supplementary Data, Table S3, the main function of the paratungstate anion is a charge balancing species for the organic or metal-organic or inorganic cations. In addition the polyanion can also function like an O-donor ligand as reported earlier for heptamolybdates[48,49] and bind to metal ions[27,28,50-55]. Compounds **1** and **2** described in this work are two new examples of organic ammonium paratungstates and the role of the polyanion is only charge balancing.

Conclusions

In this study, two new organic ammonium paratungstates viz. $(MeNH_3)_{10}[H_2W_{12}O_{42}]\cdot12H_2O$ **1** and $(EtNH_3)_{10}[H_2W_{12}O_{42}]\cdot4H_2O$ **2** have been synthesized and structurally characterized by the exploration of the tungsten trioxide /amine/water reaction system for several organic amines. Although the clear reaction mixture which is alkaline contains $(WO_4)^{2-}$ anion as confirmed by Raman spectral studies, our efforts to isolate the tetrahedral tetraoxidotungstate(VI) species charge balanced by organic ammonium cations have not been fruitful. Slow evaporation of the reaction mixture resulted in its transformation to paratungstate anion as confirmed by Raman spectral studies. Efforts to crystallize other organic paratungstates and study their crystal structures are currently underway in our laboratories.

Supplementary Data

Deposition Numbers CCDC 2016772 (for **1**) and CCDC 2016773 (for **2**), contain the supplementary crystallographic data for this paper. These data are provided free of charge by the joint Cambridge Crystallographic Data Centre and Fachinformationszentrum Karlsruhe Access Structures service www.ccdc.cam.ac.uk/structures. Supplementary Data (Tables S1-S3, Scheme S1 and Figs S1-S5) associated with this article are available in the electronic form at http://nopr.niscair.res.in/jinfo/ijca/IJCA_60A(02)185-195_SupplData.pdf.

Acknowledgement

The authors thank the Sophisticated Analytical Instrument Facility, Indian Institute of Technology, Madras for the single crystal X-ray structure determination of **1** and **2** reported in this paper. Financial assistance to the School of Chemical Sciences (formerly Department of Chemistry), Goa University at the level of DSA-I under the Special Assistance Programme (SAP) by the University Grants Commission, New Delhi is gratefully acknowledged**.** SMM is a recipient of the UGC-NFO Fellowship by UGC, New Delhi *vide* letter F./2015-16/NFO-2015-17-OBC-GOA-26835/(SA-III/Website).

References

1 Greenwood N N & Earnshaw A, *Chemistry of the elements* (Pergamon press, Oxford) 1984. For Scheele's report on tungsten see https://babel.hathitrust.org /cgi/pt?id =nnc 1.cu61255840&view=1up&seq=7

2 Wöhler F, *Ann Phys*, 2 (1824) 345. For an English translation of this paper see Wöhler F, *Phil Mag*, 66 (1825) 263.

3 Lotz W, *J Prakt Chem*, 63 (1854) 209.

4 Scheibler C, *J Prakt Chem*, 83 (1861) 273.

5 Marignac C, *Ann Chim Physique*, 69 (1863) 5.

6 Gibbs W, *Amer Chem Journ*, 1 (1879) 218.

7 Rosenheim A, *Z Anorg Chem*, 96 (1916) 139.

8 Smith E F, *Chem News*, 129 (1924) 198.

9 Souchay P, *Ann Chim*, 18 (1943) 61.

10 Vallance R H, *J Chem Soc*, (1931) 1421.

11 Saddington K & Cahn R W, *J Chem Soc*, (1950) 3526.

12 Sturdivant J H, *J Am Chem Soc*, 59 (1937) 630.

13 Grűttner B & Jander G, in Handbook of preparative inorganic chemistry, (Edited by Brauer G) Vol 2 (second edition) 1962, 1698.

14 Cotton F A, Wilkinson G, Murillo C A & Bochmann M, *Advanced Inorganic Chemistry,* 6th Ed. (Wiley Interscience publication) 1999.

15 Pope M T & Müller A, *Angew Chem Int Ed Engl*, 30 (1991) 34.

16 Nadal L V & Cronin L, *Nature Rev,* 2 (2017) 1.

17 Kumar T, Bhoi U, Naulakha P & Das S K, *Inorg Chim Acta*, 506 (2020) 119554.

18 Wutkowski A, Srinivasan B R, Naik A R, Schütt C, Näther C & Bensch W, *Eur J Inorg Chem,* (2011) 2254

19 Ma P, Hu F, Wang J & Niu J, *Coord Chem Rev,* 378 (2019) 281.

20 Tewari S, Adnan M, Balendra, Kumar V, Jangra G, Prakash G V & Ramanan A, *Front Chem*, 6 (2019) 631.

21 Lindqvist I, *Acta Crystallogr*, 5 (1952) 667.

22 Lindqvist I, *ArkivKemi,* 2 (1950) 325.

23 Lipscomb W N, *Inorg Chem*, 4 (1965) 132

24 Weiss V G, *Z Anorg Allg Chem*, 368 (1969) 279.

25 Allmann V R, *Acta Crystallogr*, B27 (1971) 1393.

26 Evans J H T. & Prince E, *J Am Chem Soc*, 105 (1983) 4838.

27 Tsay Y H & Silverton J V, *Z Kristallogr Cryst Mater,* 137 (1973) 256.

28 Gumerova N I, Dobrov A, Roller A & Rompel A, *Acta Crystallogr*, C74 (2018) 1252.

29 Groom C R, Bruno I J, Lightfoot M P & Ward S C, *Acta Crystallogr*, B72 (2016) 171.

30 Belsky A, Hellenbrandt M, Karen V L & Luksch P, *Acta Crystallogr,* B58 (2002) 364.

31 Srinivasan B R & Morajkar S M, *Indian J Chem*, 55A (2016) 676.

32 Maksimovskay R I & Burtseva K G, *Polyhedron*, 4 (1985) 1559.

33 Yan G, Wang X, Ma Y, Cheng X, Wang Y & Li Y, *Solid State Sci*, 17 (2013) 146.

34 Jeannin Y P, *Chem Rev*, 98 (1998) 51.

35 Feng Y Q, Huang Q Z, Qiu D F & Meng Z H, *Russ J Coord Chem,* 36 (2010) 544.

36 Morajkar S M & Srinivasan B R, *Indian J Chem*, 59A (2020) 1760.

37 Altomare A, Cascarano G, Giacovazzo C, Guagliardi A, Burla M C, Polidori G & Camalli M, *J Appl Crystallogr,* 27 (1994) 435.

38 Sheldrick G M, *Acta Crystallogr,* C71 (2015) 3.

39 Khandolkar S S, Naik A R, Näther C & Bensch W, *J Chem Sci,* 128 (2016) 1737.

40 Nakamoto K, *Infrared and Raman spectra of Inorganic and coordination compounds part A: Theory and Applications in Inorganic Chemistry* 6th ed. (John Wiley, New Jersey) 2009.

41 Tanisaki S, *J Phys Soc Jpn*, 15 (1960) 573.

42 Tanisaki S, *J Phys Soc Jpn*, 11 (1956) 620.

43 Gerand B, Nowogrocki G, Guenot J & Figlarz M, *J Solid State Chem*, 29 (1979) 429.

44 Reis K A, Ramanan A & Whittingham S, *Chem Mater*, 2 (1990) 219.

45 Wells A F, *Structural Inorganic Chemistry* 4th ed. (Oxford University Press, London/ New York) 1975, p. 474.

46 Mote K R, Thomas J & Ramanan A, *Indian J Chem*, 57A (2018) 1081.

47 Desiraju G R, Vittal J J & Ramanan A, *Crystal Engineering – A Textbook*, (World Scientific, Singapore) 2011.

48 Srinivasan B R, Khandolkar S S & Morajkar S M, *Indian J Chem*, 59A (2020) 517.

49 Srinivasan B R, Morajkar S M, Khandolkar S S, Näther C & Bensch W, *Indian J Chem*, 56A (2017) 601.

50 Lisnard L, Dolbecq A, Mialane P, Marrot J & Secheresse F, *Inorg Chim Acta*, 357 (2004) 845.

51 Yan B, Goh N K & Chia L S, *Inorg Chim Acta,* 357 (2004) 490.

52 Kong Q J, Zhang C J & Chen Y G, *J Mol Struc,* 964 (2010) 82.

53 Shi D, Yu H, Pang H & Chen Y, *Solid State Sci*, 10 (2008) 847.

54 Li Y W, Wang Y H, Li Y G, Wang E B, Chen W L, Wu Q & Shi Q, *Inorg Chim Acta*, 362 (2009) 1078.

55 Qu X, Yang Y, Yu X, Lv Z, Ji M & Feng S, *Inorg Chem Commun*, 60 (2015) 126.